METHODS FOR LWIR RADIOMETRIC CALIBRATION AND CHARACTERIZATION

Robert Ryan[a*], Mary Pagnutti[a], Vicki Zanoni[b], Gary Harrington[a], Dane Howell[a], Randy Stewart[a]

[a] Remote Sensing Directorate, Lockheed Martin Space Operations – Stennis Programs, Bldg. 1105, SSC, MS 39529 – (robert.ryan, mary.pagnutti, gary.harrington, dane.howell, randy.stewart)@ssc.nasa.gov
[b] NASA Earth Science Applications Directorate, Bldg. 1100, SSC, MS 39529 – vicki.zanoni@ssc.nasa.gov

Commission I, Working Group I/2

KEY WORDS: Radiometric, Temperature, Accuracy, Thermal, Polarization

ABSTRACT:

The utility of a thermal remote sensing system increases with its ability to retrieve surface temperature or radiance accurately. Several applications require absolute or relative accuracies far better than 1 °C. To achieve these levels of accuracy routinely, scientists must perform laboratory and onboard calibration as well as in-flight vicarious characterization, incorporating a well-calibrated infrared radiometer that is mounted on a buoy and placed on a uniform water body. The radiometer monitors the water surface radiant temperature. Combining this measurement with atmospheric pressure, temperature and water vapor profiles, a top-of-the-atmosphere radiance estimate can be calculated with a radiative transfer code to compare with the sensor's output. On very still waters, however, a buoy can significantly disturb these measurements. Scientists at NASA's Stennis Space Center (SSC) have developed a novel approach, using an uncooled infrared camera mounted on a boom, to quantify buoy effects. Another critical aspect of using boom-mounted infrared radiometers is the need for extensive laboratory characterization of the instruments' radiometric sensitivity, field of view and spectral response. Proper water surface temperature also requires a detailed knowledge of both the upward emission and reflected sky emission. Recent work at SSC has demonstrated that the use of a polarization-based radiometer, operating at the Brewster angle, can simplify temperature retrieval as well as improve overall accuracy.

1. INTRODUCTION

The NASA Earth Science Applications (ESA) Directorate is responsible for developing and validating applications using NASA's remote sensing technologies. One of these technology areas, multispectral thermal infrared imaging, is an active area of research that has many applications (Jensen, 2000). A major challenge for a thermal imaging system is the ability to provide accurate temperature assessments due to drift of onboard radiometric calibration sources and optical component contamination. Since some applications such as climate modeling using sea surface temperature measurements require accuracies approaching 0.1–0.2 °C, the ability to routinely characterize such systems is critical (Robinson et al., 1984).

A common technique for characterizing the radiometric performance of an infrared system is to image a well-characterized large infrared source with high emissivity and uniform temperature. By combining surface temperature measurements with atmospheric profiles, an accurate at-sensor radiance estimate can be calculated using Moderate Resolution Transmittance (MODTRAN) or other radiative transfer codes. With enough at-sensor radiance estimates, a vicarious calibration can be performed. This calibration can be used to augment or replace any onboard calibration method.

Water in the infrared (8-14 μm) has an emissivity approaching unity thus approximating a good blackbody (Horwitz, 1999). Water bodies that are at least several meters deep after a disturbance, thermally vertically stratify while becoming relatively uniform horizontally. Large water surfaces such as deep lakes can be uniform to more than 1 °C over several hundred meters. Averaging spatially or repeating measurements can reduce the effective variation to a small fraction of this value. These two characteristics make man-made and large natural lakes potentially excellent infrared remote sensing systems calibration sources.

Unfortunately there can be a 1 °C or more temperature difference between the surface and bulk temperature, making use of conventional kinetic temperature thermometers problematic (Katsaros, 1979). Additionally, since 99 percent of infrared radiation is absorbed in the first 100 μm of the water layer, remote sensing systems measure skin temperature and not bulk temperature (Horwitz, 1999). This difference in temperature between bulk and skin is primarily due to convection and evaporation occurring at the surface. These conditions will generate a bias in any comparison with remote sensing results that will not average out.

Because of these characteristics of water bodies, ground-based verification and calibration of infrared systems are often accomplished via ship or buoy-mounted infrared radiometers placed in the water body (Donlon et al., 1998; Smith et al., 1995). These infrared radiometers measure the surface temperature. NASA SSC has adopted this approach and has developed a deployable float (buoy) that is used at the SSC High Pressure Industrial Water Reservoir (HPIWR). The HPIWR is approximately 200 m in diameter and 10 m deep. It is an artificial reservoir used to provide water cooling for rocket engine tests. The HPIWR and the SSC float have been used to characterize the Department of Energy's (DOE) Multispectral Thermal Imager (MTI) and the NASA Airborne Terrestrial Applications Sensor (ATLAS) (Fowler, 1995; Pagnutti, 2002).

* Corresponding author.

This paper addresses the basic principle of these types of measurements, associated errors, and methods and procedures used to maximize the accuracy of such measurements.

We begin with a discussion of the general issues associated with choosing a water body, platform design and radiometry fundamentals. We follow with sections that describe specific approaches that NASA SSC and other groups have taken to address the above issues.

2. WATER BODY SELECTION

The selection of the water body is critical for the ultimate success of a calibration effort. At SSC, we have focused on small water bodies that can be a few hundred meters in length in any direction. We are working with relatively small Ground Sample Distance (GSD) systems, which increase the number of sources. This is an important consideration for a deployable calibration source such as the SSC float, which is also planned to be used to support thermal projects at remote sites. Our float is designed to be launched like a small boat at a boat ramp and can be towed to a desired location.

A rule of thumb is that the water body should be at least 5-10 pixels in extent, in any direction, to minimize errors associated with adjacency effects associated with a finite Point Spread Function. Adjacency effect errors can be significant if the temperature difference between the water body and the surrounding land area is large and the water body is not large enough, compared to the spatial resolution of the system, to have pure pixels in the measurement region. At several pixels in size, adjacency effects are typically less than 0.1 ^{o}C.

The uniformity of the water body should also be characterized to ensure that there are minimal variations due to natural springs or other thermal disturbances. An excellent way to characterize the uniformity of a potential target is to acquire high-spatial resolution thermal imagery. In many cases, the sensor being characterized can be used. We have used ATLAS imagery at 2.5-m GSD to examine the SSC HPIWR. Sample visible and thermal imagery are shown in Figure 1. The thermal image is converted to temperature and a water mask is used to show only water. The root mean square (RMS) temperature variation across the surface was shown to be less than 0.5 ^{o}C. A small warm water spring can be noticed in the lower region of the thermal image.

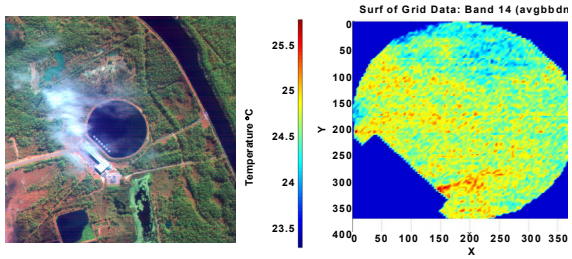

Figure 1. ATLAS visible and thermal imagery of the SSC HPIWR reservoir

3. PLATFORM CONSIDERATIONS

On water bodies that do not have significant wave action, the platform and the way it is moored and constructed can cause significant influences on the surface temperature surrounding the buoy. Acquiring data off axis offers logistic advantages, enabling shore-based radiometry and off-axis viewing from ships or buoys minimizes platform disturbances. In general, off-axis viewing increases the sky emission seen by the radiometer and the polarization of the signal. These considerations are discussed in subsequent sections.

Initial testing of the early float produced varied results. Initial work at SSC with the Department of Energy Savannah River Test Site group examined a three-point float using three cubes of styrofoam to support the instrumentation. Ropes were used to secure the float to a fixed position. Using an Inframetrics SC2000 uncooled microbolometer infrared camera mounted on a large crane shown in Figure 2, high-spatial resolution imagery was acquired of the float at its deployed location.

Figure 2. Crane used to position thermal camera over float

The rope's influence in the water shown in Figure 3 was easily seen, even though the ropes were greater than 15 cm below the surface. Temperature disturbances as much as 1 ^{o}C were observed. NASA SSC changed to a pontoon design similar to JPL floats used in Lake Tahoe. Examining the platform disturbances with the crane mounted infrared camera, it was found that at times, a 0.5 ^{o}C difference existed between the "upstream" and "downstream" temperatures. To correct for the change in temperature "downstream" of the float, two radiometers were set at opposing booms to ensure at least one would always provide water temperatures unaffected by the float disturbances. The radiometers were also set to look at 15 degrees off nadir to increase the physical offset between the measurement region and the float. A photograph of the float, as presently configured, is shown in Figure 4.

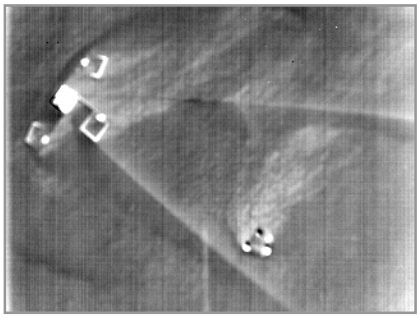

Figure 3. Early float designs showing the influence of the float and mooring on measurements.

In addition to two downward looking radiometers, there are several other instruments aboard the float that measure air temperature, bulk water temperature, wind speed and direction, and downwelling radiation. These additional measurements are used to support data analysis and check consistency of the surface temperature measurements.

Figure 4. SSC thermal calibration float

4. RADIOMETRY

Figure 5 shows a typical radiometer configuration and radiation sources for small distances in an atmospheric window. Monochromatic radiance incident on a radiometer for a near specular source, such as water at normal incidence, can be described by expression (1). At near normal incidence, polarization effects are minimal. Neglecting self-viewing, the spectral radiance $R(\lambda)$ measured by the sensor at wavelength λ for a water body with surface temperature T_s is given by

$$R(\lambda) = \varepsilon(\lambda)B(\lambda, T_S) + (1 - \varepsilon(\lambda))S_{\downarrow}(\lambda) \qquad (1)$$

where $B(\lambda, T_S)$, $\varepsilon(\lambda)$, and $S_{\downarrow}(\lambda)$ are the Planck function, surface emissivity, and down-welling radiation, respectively.

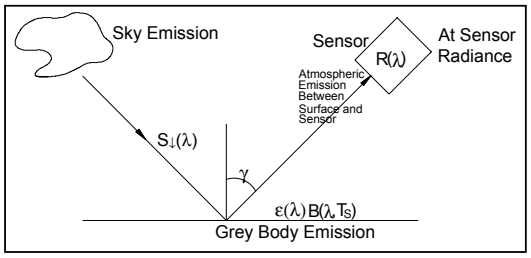

Figure 5. Typical radiometer configuration and radiation sources

Most sensors integrate over a spectral region and measure a weighted average radiance $\overline{R}$ due to the sensor spectral responsivity $f(\lambda)$, given by

$$\overline{R} = \int_{\lambda_1}^{\lambda_2} f(\lambda)R(\lambda)d\lambda \qquad (2)$$

This integrated response is then related to the equivalent blackbody temperature through a calibration curve that is generated by observing a high quality blackbody.

The sources of error (excluding calibration errors) include uncertainty in water surface emissivity, $\delta\varepsilon(\lambda)$, and uncertainty in downwelling sky radiation, $\delta S_{\downarrow}(\lambda)$. In practice, water surfaces are neither pure nor perfectly flat. Waves and impurities typically increase the emissivity. Measurements of sea surfaces show emissivity uncertainties of 0.25 percent or less, which correspond to temperature errors of 0.1 ^{o}C or less (Masuda et al., 1988). In the presence of impurities such as surfactants, the emissivity error can be larger. Uncertainties in downwelling sky radiation are generally due to errors in the water vapor and temperature profiles of the atmosphere and can be significantly reduced using radiosonde data. Unfortunately, launching radiosondes is not always practical. The uncertainty without radiosonde measurements due to variations in the atmosphere lead to surface temperature errors on the order of 0.1 ^{o}C, which can grow to 0.4 ^{o}C when clouds are present at near normal incidence. Off-axis viewing significantly increases these errors. This will be discussed in more detail in Section 5. Other sources of error are instrument noise and calibration errors, which can cause uncertainties of 0.1 ^{o}C for good radiometers.

The total expected accuracy, σ_T, can be estimated with the following expression

$$\sigma_T = \sqrt{\sigma_{T_\varepsilon}^2 + \sigma_{T_{sky}}^2 + \sigma_{T_{sensor}}^2} \qquad (3)$$

where σ_{T_ε}, $\sigma_{T_{sky}}$, and $\sigma_{T_{sensor}}$ are the uncertainty in the surface temperature due to uncertainty in emissivity, sky emission, and sensor calibration and noise. The major uncertainty in estimating skin surface temperature is driven by the presence of clouds or lack of knowledge of sky emission. Even with a clear sky, current techniques will only achieve about 0.2 ^{o}C skin surface accuracy. This does not include any error that would result from optics becoming contaminated in the field and the uncertainty in the atmosphere.

4.1 Surface Temperature Measurements with Broadband Radiometers

To keep the cost of such a system down, we have chosen to use commercially available broadband Heimann KT15D 8-14 µm radiometers. These radiometers are also used by several other groups. The Heimann KT15D radiometer is a pyroelectric detector-based infrared radiometer. A lens collects infrared radiation and focuses it upon the uncooled detector. The specifications for the radiometer are: 0 to 500 °C temperature range, 3° field of view, and programmable response times. The signal is generated by chopping the scene against an internal blackbody reference. The AC signal produced is processed by a lock-in amplifier, and the output is provided either as an analog or digital signal. The sensitivity of the radiometer depends upon the integration time used in the lock-in amplifier low pass filter. It interfaces with a PC through an RS232 interface. The emissivity of the source, time constant, and radiometer temperature can be set remotely. The output (radiance temperature of the source) and radiometer temperature can be interrogated. The radiometer output is provided in radiant temperature using the manufacturer's calibration.

4.2 Radiometer Characterization

Every radiometer used is characterized in the laboratory. Specific items discussed here include warm-up characteristics, calibration corrections of the manufacturer, and environmental effects. The major characterizations are performed with a water bath blackbody (Fowler, 1995). The radiometer is pointed at an insulated, stirred water bath, with a specular blackbody cone. For our measurements, we used a Mikron Precision Water Bath Blackbody Model M385. The water bath has a temperature range of 5 to 95 °C, with a cone emissivity of approximately 0.9999 (Fowler, 1995). The water bath blackbody is instrumented with a Azonix Model A11011-RS-XX-RT41 thermometer that has a precision of 0.001 ºC and an accuracy of 0.002 ºC. This temperature probe was crosschecked with a Hart Model 1522 thermometer. The measurements agreed to within 0.005 ºC. Both the Azonix and the Heimann KT15D radiometer RS232 outputs were recorded on a laptop computer. Measurements of the water bath temperature over a 20-hour period showed less than a 0.005 ºC variation.

Since we deploy our float only for a brief period of time, it is critical to determine the warm-up characteristics. The warm-up characteristics are determined by turning the radiometer on and observing a fixed temperature water bath blackbody. Before beginning the experiment, we ensured that the radiometer had been off for several hours. The absolute difference between the radiometer and the high-precision water bath was recorded. The manufacturer defines warm-up time as 15 minutes. After 15 minutes, the radiometer should be within 0.1 ºC of the steady state offset. From our measurements we have defined the warm-up period to be 50 – 60 minutes. This period of time guarantees that the radiometer has reached its steady state value and the measurements have clearly reached a steady state condition with any uncertainties being dominated by the precision of the instrument.

Although the manufacturer provides a calibration, we found it could differ from the blackbody temperature by 0.5 ºC or more. The Heimann KT15D radiometer outputs a radiant temperature as a digital output or an analog voltage proportional to the temperature. For most of our work, we used the RS232 digital output. The calibration coefficients for each radiometer were determined by recording Heimann KT15D and water bath blackbody temperatures while the water bath temperature was ramped over 5 ºC to 45 ºC. This is the expected temperature range over which the water bodies of interest vary. Both the Azonix and the Heimann KT15D radiometer RS232 outputs were recorded on a laptop computer and written to a text file. We determined there is a small offset of approximately 0.3 ^{o}C over a large portion of the calibration range. A polynomial fit is then used to correct the radiometers' output. Applying a new set of calibration coefficients, the RMS calibration error is reduced to less than 0.1^{o}C.

Further testing of the radiometer in extreme temperature conditions exposed a potential for error in measurements. Radiometer calibrations could drift by as much 1 ^{o}C for some radiometers when the ambient temperature surrounding the radiometer was significantly different than the laboratory calibration temperature. We noticed anomalies on occasions when the ambient temperature was significantly different from the 20 ^{o}C laboratory calibration temperature. We placed radiometers in an environmental chamber and ran calibrations at different case temperatures. We chose 40 ^{o}C, since this is about the approximate maximum ambient temperature experienced on the HPIWR. Figure 6 shows the effect of ambient temperature on radiometer calibrations for two different radiometers.

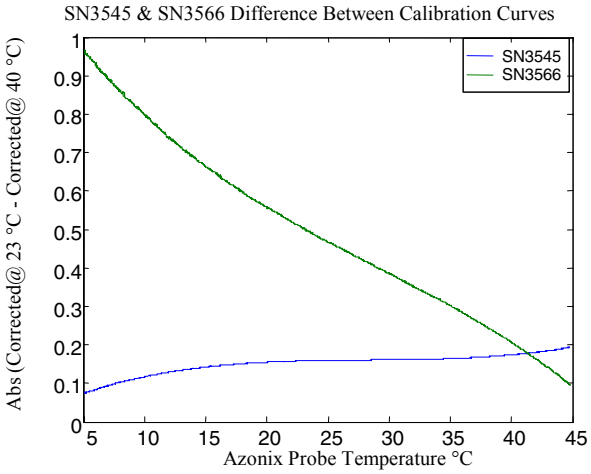

Figure 6. Effects of ambient temperature on calibration coefficients

To minimize environmental effects, the radiometer was enclosed in a heated housing with the exception of the front of the optics and stabilized to 40 °C. By temperature stabilizing the radiometer, laboratory calibrations can be more easily transferred to the field.

In addition to temperature stabilizing the radiometers, the float contains ambient temperature blackbodies that are extended in front of the radiometers every several minutes and used to check the temperatures observed by the radiometers. The ambient temperature blackbodies were built using Eppley high-emissivity, paint-coated, copper honeycomb blackbodies. The emissivity of the blackbody has been estimated to be 0.99. The temperature of the blackbody is monitored with a Hart Model 1522 thermometer. The blackbody is housed in a shaded enclosure, similar in design to the ones used for measuring air temperature. As the air temperature drifts, these ambient temperature blackbodies serve to provide an independent calibration check over a small temperature range. We also check the radiometers with field portable water bath blackbodies built around an ice chest before and after the collect (Donlon et al., 1999). An anodized aluminum cone is attached to a water-filled ice chest that uses a submersible pump to stir the water. The water temperature is monitored with a Hart Model 1522 thermometer. We typically use two homebuilt blackbodies with water temperatures that bound the expected observed water surface temperature extremes for a given collect.

5. SPECTROPOLARIMETER MEASUREMENTS

Ground validation techniques with high accuracies require analysis and optimization of the radiometer's spectral bandpass, temporal and spatial resolution, viewing geometry and emissivity sensitivity. An instrument that makes both spectral and polarization measurements together could be used to discriminate graybody emission from sky emission to enable better than 0.1 ^{o}C accuracy. The ESA Directorate has developed a novel infrared spectropolarimeter for measuring high spectral resolution (approximately 8 cm^{-1}) infrared

emission in two or more polarizations. Unlike previous work, spectral polarization and viewing geometry have been implemented in this measurement technique. These observation parameters affect the emissivity reading for the surface in question.

For radiometer off-axis viewing geometries, atmospheric and polarization effects are more significant, thus complicating the radiative transfer. The complex Fresnel equations are used to calculate emissivity at increasing off-axis view angles for polarization effects (Masuda et al., 1988). The function, integrated over wavelengths from 8-12 µm for perpendicular and parallel polarizations, is shown in Figure 7.

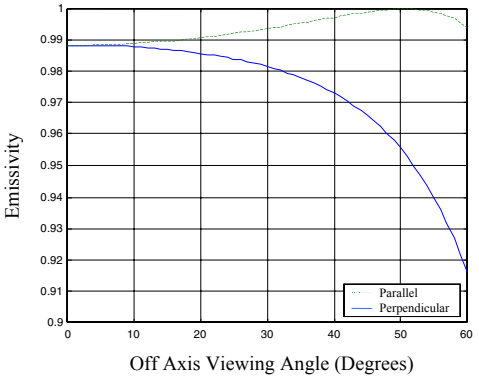

Figure 7. Effects of viewing angle on emissivity

The real and imaginary indices of refraction of water are well known over the spectral region of interest. Combining the complex Fresnel equations with Planck's equation and atmospheric models, we can model the spectrally polarized radiation, which is the basis for the radiative transfer model developed under this effort. The resulting parallel and perpendicular radiation components, which replace expression (1), are shown in the following expression.

$$R_{\|} = \varepsilon_{\|}(\lambda)B(\lambda,T_S) + (1-\varepsilon_{\|}(\lambda))S_{\downarrow}(\lambda) \qquad (4)$$
$$R_{\perp} = \varepsilon_{\perp}(\lambda)B(\lambda,T_S) + (1-\varepsilon_{\perp}(\lambda))S_{\downarrow}(\lambda)$$

where $R_{\|}$, $R_{\perp}$, $\varepsilon_{\|}$ and $\varepsilon_{\perp}$ are the polarized radiances and emissivities, respectively. Examining expression (4) with knowledge of $\varepsilon_{\|}$ and $\varepsilon_{\perp}$ for pure water, $S_{\downarrow}(\lambda)$ and $B(\lambda,T_s)$ can be independently estimated by measuring $R_{\|}$ and $R_{\perp}$ without direct observation of $S_{\downarrow}(\lambda)$.

The spectral region was limited to minimize atmospheric errors. The spectral structure due to atmospheric absorption also increases with view angle. The uncertainties in downwelling radiation and emissivity increase as an instrument views from off axis. These errors, as mentioned above, can exceed 1 ^{o}C. Note that near the Brewster angle, the emissivity for the parallel polarization approaches unity. For this geometry and polarization, sky emission reflectances are minimized. By implementing both spectral and polarimetric measurement techniques, these biases can be minimized through analysis or sensor optimization.

To explore the various methods mentioned above for improving the performance of infrared radiometers, a commercial Midac Fourier Transform Infrared Spectrometer (FTIR) was modified. The Midac FTIR is a high-quality spectrometer with 1 cm^{-1} resolution, covering the 2-15 µm spectral region. The high-spectral resolution provided by the FTIR supports spectral bandpass design and optimization. The FTIR by itself is not a polarimetric radiometer. The addition of foreoptics, polarizers, a scan mirror, and blackbody sources enable the spectrometer to measure radiometric polarized signals. The foreoptics are used to control the field of view of the instrument. The polarizer selects a specific polarization for detection. For each measurement, the polarizer is set and the scan mirror points the system at blackbody sources to calibrate for various measurements.

A prototypical system, based on a Midac FTIR and a Molectron wire grid polarizer, was constructed. The experimental setup consists of two rotational stages, one for a gold steering mirror and the other for the polarizer. The gold mirror rotational stage directs the beam at blackbody reference sources (hot and cold) and a water body for data collection. The instrument was calibrated against two water bath blackbodies for both parallel and perpendicular polarizations. Analysis of emission versus off-axis viewing angles of water demonstrates the benefit of polarization. At the Brewster angle the parallel polarization emissivity approaches unity, virtually eliminating any reflected radiation off the water surface.

The spectropolarimeter was tested in the laboratory environment, with the instrument positioned to view a water source at the Brewster angle. The water was gently stirred with a bilge pump, and a precision thermistor measured the water temperature. A hot 150 °C blackbody was arranged so its radiation was reflected off the water. This blackbody source, mimicking a cloud overhead during a field exercise, will produce approximately a 7 percent radiometric error at normal incidence and up to 25 percent near the Brewster angle for the perpendicular polarization. This high-temperature source was used to magnify the polarization sensitivity effects. The polarizer rotational stage functions as a means to develop perpendicular and parallel measurements of the surface emission of water.

The water surface emission was measured in the laboratory using both perpendicular and parallel polarizations. Figure 8 shows the water graybody emission and reflected high-temperature blackbody at the Brewster angle for perpendicular polarization, along with a theoretical blackbody curve derived from the thermistor measurements. It is evident that, in this arrangement, significant radiation is being reflected off the water surface.

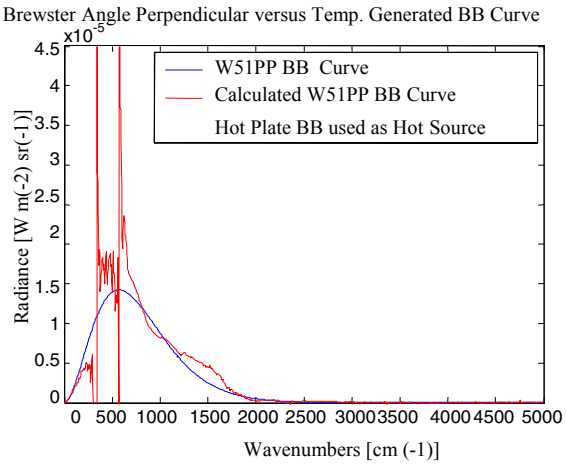

Figure 8. Theoretical room temperature water graybody emission versus measured water body emission using perpendicular polarization

Figure 9 shows the same curves from Figure 8, but at the angle for parallel polarization. It can be seen that, in the parallel polarization arrangement, the reflected signals have been severely attenuated, leaving only the water graybody emission.

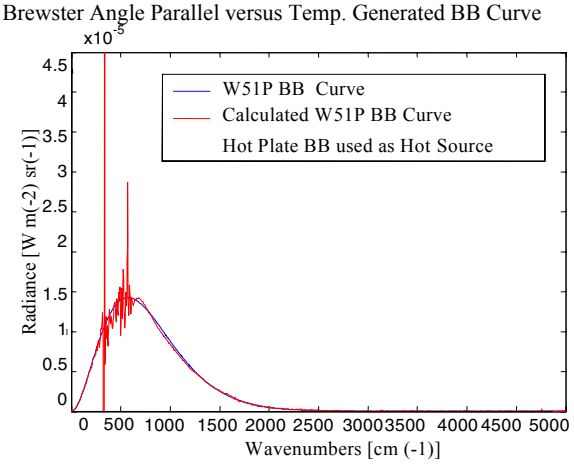

Figure 9. Theoretical room temperature water graybody emission versus measured water body emission using parallel polarization

In Figure 8, most of the spectrum shows nearly a 10-20 percent increase in signal due to the reflected radiation in the perpendicular polarization. We have observed that a small part of the spectrum reverses. This anomaly is being explored and may be due to emissivity, surfactant effects, or calibration errors.

These measurements demonstrate that the exploitation of polarization through the spectropolarimeter design can result in improvements over traditional radiant temperature measurements for remote sensing. This device can potentially enable polarization and spectral trades covering the 3-5 µm and 8-14 µm spectral windows.

Future activities will improve the blackbodies' calibration. This is an area that could be explored in the next generation system. Further work should be performed to test the spectropolarimeter in the field, and to deploy and operate the spectropolarimeter simultaneously with a well-characterized floating radiometer in order to compare the instrument results with independent radiometer measurements. Radiosondes should also be launched and software model estimates made and compared with the spectropolarimeter measurements.

6. SUMMARY

The general issues for characterization of infrared systems have been presented as well as a discussion on a new spectropolarimetric device for potential better accuracies. The spectropolarimeter will permit polarized measurements of infrared radiation at very high spectral resolutions. With this instrument, SSC and the ESA Directorate have the capability to conduct spectral and polarimetric trade studies for improved infrared radiometer measurements and thermal infrared applications validation.

REFERENCES

Donlon, C., Keogh, S., Baldwin, D., Robinson, I., Ridley, I., Sheasby, T., Barton, I., Bradley, E., Nightingale, T., Emery, W., 1998. Solid State Radiometer Measurements of Sea Surface Skin Temperature. *Journal of Atmospheric and Oceanic Technology (J. Atmos. Ocean. Technol.)*, 15(3), pp. 775-787.

Donlon, C., Nightingale, T., Fiedler, L., Fisher, G., Baldwin, D., Robinson, I., 1999. The Calibration and Intercalibration of Sea-Going Infrared Radiometer Systems Using a Low- Cost Blackbody Cavity. *Journal of Atmospheric and Oceanic Technology*, 16, pp. 1183-1197.

Fowler, J., 1995. A Third Generation Water Bath Based Blackbody Source. *Journal of Research of the National Institute of Standards and Technology*, 100(5), pp. 591-599.

Horwitz, J., 1999. Water at the ice point: a useful quasi-blackbody infrared calibration source. *Applied Optics*, 38(19), pp. 4053-4057.

Jensen, J., 2000. *Remote Sensing of the Environment*. Prentice Hall, Inc., Upper Saddle River, NJ, pp. 243-283.

Katsaros, K., 1979. The Aqueous Thermal Boundary Layer. *Boundary-Layer Meteorology*, 18, pp. 107-127.

Masuda, K., Takashima, T., Takayama, Y., 1988. Emissivity of Pure and Sea Waters for the Model Sea Surface in the Infrared Window Regions. *Remote Sensing of Environment*, 24, pp. 313-329.

Pagnutti, M., et al., 2002. "Multispectral Thermal Imager Characterizations at the John C. Stennis Space Center."

Robinson, I., Wells, N., Charnock, H., 1984. Review Article: The sea surface thermal boundary layer and its relevance to the measurement of sea surface temperature by airborne and space borne radiometers. *International Journal of Remote Sensing*, 5(1), pp. 19-45.

Smith, W., Kneteson, H., Feltz, W., Howell, H., Menzel, W., Nalli, N., Brown, O., Brown, J., Minnett, P., McKeown, W. 1995. Observations of the Infrared Radiative Properties of the

Ocean-Implications for the Measurement of Sea Surface Temperature via Satellite Remote Sensing. *Bulletin of the American Meteorological Society*, 77(1), pp. 41-51.

ACKNOWLEDGEMENTS

The NASA Earth Science Applications Directorate under contract number NAS 13-650 at the John C. Stennis Space Center, Mississippi, and NASA's SSC Center Director Discretionary Funds supported this work.

Mention of particular products, companies, or agencies does not imply endorsement by the U.S. Government, NASA, or Lockheed Martin Space Operations - Stennis Programs.